The Journal of Experimental Biology 216, 3015-3022

doi:10.1242/jeb.082974

RESEARCH ARTICLE

Glossosoma nigrior (Trichoptera: Glossosomatidae) respiration in moving fluid

Mark W. L. Morris* and Miki Hondzo

Department of Civil Engineering, Saint Anthony Falls Laboratory, University of Minnesota, Minneapolis, MN 55414, USA

*Author for correspondence (morri544@umn.edu)

SUMMARY

Laboratory measurements of dissolved oxygen (DO) uptake by *Glossosoma nigrior* Banks were conducted in a sealed, recirculating flume under variable fluid flow velocities. Measurements were performed in similar water temperatures, DO concentrations and fluid flow velocities to field conditions in the stream where the larvae were obtained. Total oxygen uptake by both cased larvae and corresponding cases without larvae were quantified. An increased fluid flow velocity corresponded to an increased larval DO uptake rate. Oxygen uptake by the larval cases alone was not as sensitive to changes in the Peclet (Pe) number, the dimensionless ratio of advective to diffusive DO transport, as uptake by larvae themselves. The flux of DO to larvae and their cases was up to seven times larger in a moving fluid in comparison to non-moving fluid conditions in the proximity of larvae for 0<Pe<175. A functional relationship was developed relating fluid flow and DO uptake across a larval case. According to the proposed quantitative relationship, Pe alone describes 91% of the variation in the DO flux to the larvae under variable fluid flow conditions. In response to fluid motion, larvae depicted two characteristic behavioral responses. When the ratio of advective DO transport to diffusive transport was low (Pe<87), larvae occasionally abandoned their cases or spent more time partially extended from their cases. At Pe>87, larvae typically remained in their cases. This indicates that oxygen delivery to the larvae at low Pe is insufficient to satisfy the respiratory demands of cased larvae.

Key words: *Glossosoma*, dissolved oxygen, respiration, flux, discharge velocity.

Received 13 November 2012; Accepted 11 April 2013

INTRODUCTION

One of the major factors controlling macroinvertebrate spatial distribution on the stream bed is the fluid flow environment surrounding them. Moving fluid potentially mediates the metabolic need of macroinvertebrates including nutrient and dissolved oxygen (DO) supply. This is apparent because many aquatic insects indirectly indicate local DO concentrations by changing their location in space and time on a stream bed. Lavandier and Capblancq reduced DO in a stream during the day at 10°C and reported large increases in macroinvertebrate drift rate at about $4\,mg\,l^{-1}$ DO concentration (Lavandier and Capblancq, 1975). Some insects have lost their ability to ventilate and have come to rely entirely on the water current to deliver DO to them (Hynes, 1970). Rheophilous Ephemeroptera, for example, are confined to running water by their respiratory physiology (Fenoglio et al., 2008). Other mayflies move their gills in low flow to facilitate the supply of DO (Eastham, 1939; O'Donnell, 2009). Additionally, nymphs of multiple mayfly genera were reported in more exposed positions on cobbles and exhibited abdominal positioning by holding their bodies off the substrate at lowered DO concentrations (Wiley and Kohler, 1980). The presence of a second macroinvertebrate order, Plecoptera, was correlated with velocity magnitude and oxygen renewal rates in summer but not in winter because of the warmer temperature and low DO in summer (Genkai-Kato et al., 2005). Genkai-Kato and colleagues specify that this behavior was not due to an oxygen gradient as DO concentrations did not differ between deep and shallow sampling points in winter or summer (Genkai-Kato et al., 2005). Rather, given a certain DO concentration, the stonefly moves until it can achieve its necessary critical oxygen supply (DO × current velocity) (Genkai-Kato et al., 2005). Many members of a third macroinvertebrate order, Trichoptera, undulate their body inside their cases to create an oxygen supply current (Okano and Kikuchi, 2012). In fact, body undulations decrease as fluid flow velocity increases (Feldmeth, 1970).

Larvae of the above-mentioned order, the caddisflies, have earned the moniker 'underwater architects' through their construction of mobile cases and filtration nets (Wiggins, 2004). Case morphology varies greatly between genera, has been a topic of investigation and, in at least one species, *Dichosmechus gilvipes*, has been shown to provide a functional advantage as larvae mature through different instars (Limm and Power, 2011). It has been noted by multiple studies that constructing and repairing cases is energetically expensive (Kwong et al., 2011; Statzner and Doledec, 2011).

Cases built by another member of the Trichoptera, *Glossosoma* spp., are well adapted for life in fast-moving fluid. *Glossosoma nigrior* construct cases of rock, fastened together by a silk that they secrete. This rock armor may contribute to the success of *G. nigrior*, which outcompete other, more vulnerable soft-bodied macroinvertebrates that utilize the same resources but do not build cases (McNeely et al., 2007). Therefore, *G. nigrior* can have a large impact on energy and nutrient flow through aquatic ecosystems (Kohler and Wiley, 1997). Furthermore, gaps in *G. nigrior* cases enhance water exchange efficiency, which is important for the pupal stage (Wiggins and Wichard, 1989). Their bluff-bodied, oblong–hemispherical stone cases may, however, work to their disadvantage in slow-moving fluid. Kovalak observed that at high water temperature and low current velocities, *G. nigrior* positioned themselves on more exposed surfaces

of bricks, indicating that *G. nigrior* uses positioning to satisfy respiratory requirements (Kovalak, 1976). At higher temperatures, saturated water contains less oxygen, but as temperature increases, *G. nigrior* respiration demands increase.

The positioning of *G. nigrior* on the stream bed has historically been thought to be a function of oxygen supply and demand, current velocity and food availability (Kovalak, 1976). The risk of predation by predominantly day-feeding sculpin was not a factor in *Glossosoma* positioning, but larval hunger level and food density were (Kohler and McPeek, 1989). Regarding food availability, *G. nigrior* inhabited fast riffles to exploit the diatoms that colonize silt-free surfaces (Scott, 1958). However, although *G. nigrior* larvae feed predominantly on diatoms, they are non-selective with regard to the type and size of diatom particle ingested (Tindall and Kovalak, 1979). Non-selective feeding may be the optimal strategy for species that show large changes in diel and seasonal microdistribution controlled by factors other than food type and availability (Tindall and Kovalak, 1979).

Given *Glossosoma*'s ecological significance, understanding the mechanisms behind their spatial distribution and population success would be valuable. Because *G. nigrior* depend on cuticular respiration, it follows that they need to be in a location where oxygen is delivered to them by the flow in order to maintain a high concentration gradient across their permeable integument. Furthermore, *Glossosoma* do not undulate their abdomens, and larvae readily abandon their cases if damaged and rebuild from scratch (Okano et al., 2010). Furthermore, the glossosomatid case impedes larval access to DO and is abandoned in low fluid flow velocities (Okano and Kikuchi, 2012). More specialized research is necessary to determine the function of the dome-shaped case (Okano et al., 2010). The effect of moving fluid on the uptake of DO by organism can be quantified by the established principles in fluid mechanics, including dimensionless numbers that integrate different modes of mass transport in moving and stagnant fluids.

This study investigated the role of the larval case and larval DO consumption rate under different fluid flow environments in order to help explain the mechanism governing larval spatial distribution on the stream bed. The objective of this study was to determine oxygen consumption of larval *G. nigrior* under controlled but varying fluid flow velocities. To address this question, we manipulated fluid flow velocity and monitored DO concentration in a laboratory setting where environmental variables such as light, velocity, temperature and DO can be controlled. We hypothesized that fluid flow mediates DO uptake by cased larval caddisflies and determines larval presence in their cases. This has implications for the mechanism underlying larval positioning on the stream bed, drift behavior and the role of the larval case. We investigated the lower extreme of flow conditions that larvae experience in their natural habitat. Note that *G. nigrior* in this study refers to the mobile larval instars, not to pupae or the imago.

MATERIALS AND METHODS

Field reference conditions

Larvae were collected from Valley Creek at the Belwin Conservancy in Minnesota during the late summer months of 2012. This perennial trout stream has a watershed of ~161 km^2, but with only 45 km^2 contributing to stream drainage (Zimmerman and Vondracek, 2007). The reference sites consisted of two ~8 m length riffles in a forested reach near the headwaters where the stream was still first order. Prior to laboratory measurements, a 60 Hz side-looking Vectrino acoustic-Doppler velocimeter (Nortek AS, Rud, Norway) was deployed to measure the variability of stream velocities in the proximity of the stream bed. One example of stream velocity, aligned with the mean downstream flow direction, that the larvae were likely to experience is depicted in Fig. 1. In this figure, z is the distance above the substrate, z_c is the roughness crest elevation, l_c is an empirically derived length scale related to fluid flow below z_c (Raupach et al., 1996; Nikora et al., 2007), $\langle u \rangle$ is the velocity evaluated at z_c, and $\langle u^* \rangle$ is the shear velocity calculated from the Reynolds stress profile (Nikora et al., 2001). Field velocities were collected in December of 2010 in a riffle ~5 m from the downstream larval collection site. The spatially averaged (over the stream bed) and time-averaged linear velocity distribution depicted well the velocity in the proximity of the stream bed (Fig. 1).

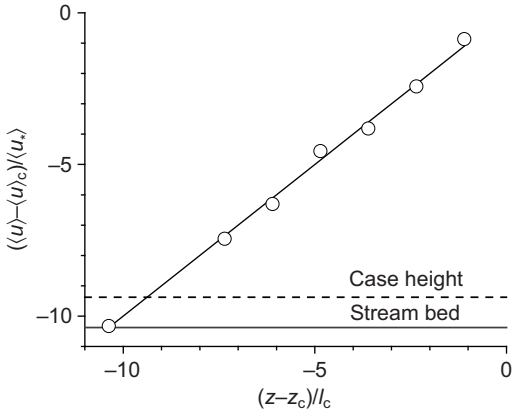

Fig. 1. Spatially averaged and time-averaged longitudinal velocity $\langle u \rangle$ profile in the proximity of the stream bed at Valley Creek, where z is the distance above the bed, z_c is the roughness crest elevation, l_c is an empirically derived length scale related to fluid flow below z_c, $\langle u \rangle_c$ is the velocity evaluated at z_c and $\langle u^* \rangle$ is the shear velocity. Each measured stream velocity data point is a time average of 12,000 data points and a spatial average over a stream bed area of 0.2×0.2 m encompassing nine velocity time series.

The proposed linear velocity distribution was used to extrapolate the velocity at 0.3 cm above the stream bed in a region of high *G. nigrior* larval abundance. In this way we estimated a stream velocity of 0.04 m s^{-1} at a distance of 0.3 cm above the substrate. The average larval case height was 0.28 cm, based on measurements of 73 larval cases. The discharge velocity (velocity averaged over the cross-sectional area of the test section) in the experimental set up ranged from 0.001 m s^{-1} at the slowest pump setting above stagnant, to 0.062 m s^{-1} at the fastest pump rate (Table 1).

A Hydrolab DS5X Multiparameter Sonde was deployed for 3 days in each of the sampling riffles where *G. nigrior* larvae were sampled to capture the range of DO and temperature that the larvae were naturally experiencing (Fig. 2). Stream temperatures ranged from 10.7 to 15.3°C, with a mean (±s.d.) of 12.5±1.1°C. DO ranged from 8.91 mg l^{-1} (88.7% saturation) to 10.40 mg l^{-1} (101.5%) with a mean (±s.d.) of 9.61±0.35 mg l^{-1} (93%). Therefore, we conducted DO consumption tests with temperatures constant within each treatment but ranging between treatments from 11.6 to 13.3°C with a mean (±s.d.) of 12.4±0.3°C, and DO ranging from 8.82 mg l^{-1} (85.1% saturation) to 9.74 mg l^{-1} (93.7% saturation).

Respiration measurements

A recirculating chamber was constructed to measure DO uptake by larvae and their cases over time in a setting where flow velocity could be controlled (Fig. 3). The entire set up was enclosed in an incubator where temperature could be set and maintained constant

Table 1. Flow rate ($\dot{Q}$), discharge velocity (U), initial dissolved oxygen concentration (C_0) and temperature (T) in the experimental set up

Pe	$\dot{Q}$ ($m^3 s^{-1}$)	U ($m s^{-1}$)	T (°C)	C_o ($mg l^{-1}$)	J_{LC} ($mg m^{-2} s^{-1}$)	J_C ($mg m^{-2} s^{-1}$)	Consumption ($mg mg^{-1} h^{-1}$)	N
0	0	0	13.4	9.83	31.8	–	–	1
3.45	5.9×10^{-7}	0.001	12.1	9.46	112.3	48.0	12.7	3
33.65	5.9×10^{-6}	0.012	12.5	9.29	131.0	66.8	12.7	3
67.54	1.2×10^{-5}	0.024	12.4	9.20	157.8	72.0	17.0	3
105.81	1.9×10^{-5}	0.038	12.4	9.30	150.8	61.7	17.7	5
147.95	2.6×10^{-5}	0.052	12.4	9.33	213.6	75.7	27.4	5
178.37	3.1×10^{-5}	0.062	12.5	9.31	215.9	73.7	28.2	4

The variables are averaged over all replicates for each treatment. Pe is the Peclet number. The number of replicates is indicated by N. J_{LC} represents dissolved oxygen (DO) flux to larvae with their cases, and J_C is flux to cases alone. Consumption refers to DO consumption by larval tissue.

during the different flow rate treatments. There was no light in the incubator to prevent any algal photosynthesis. One of two 0.02×0.02×0.57 m acrylic chambers, closed with Tygon tubing, was filled completely with Valley Creek water filtered through a glass microfiber 0.7 µm filter. A peristaltic pump circulated the water inside the chamber. A smaller, 120 ml chamber was used for a stagnant fluid treatment in order to obtain the DO flux in conditions where molecular diffusion was more significant for delivery of DO to larvae and their cases.

Oxygen consumption was measured with a needle-type PreSens MicroxTX3 sensor (PreSens, Regensburg, Germany). The oxygen sensor was an optical DO sensor of type PSt1 with a resolving accuracy of 0.04 $mg l^{-1}$. The 90% response time was <30 s in liquid. Our measurements were taken every 30 s and smoothed with a 2 min averaging window before the DO concentration decrease over time was fitted by linear regression. Linear regression was performed with OriginPro 8.6 (OriginLab Corporation, Northampton, MA, USA) software. Larvae were held in a shallow, aerated, recirculating incubator at a controlled temperature of ~13°C through the use of a chiller. At the start of each replicate, 7–11 larvae were placed in the test section of the chamber, and subjected to specified fluid flow velocity (Table 1). The change of DO concentrations in the experimental set up was first recorded in the presence of larvae and cases together. After a satisfactory decrease in DO concentration was achieved, larvae were removed from their cases, and measurements were immediately continued in the same water and flow rate conditions. Hence, measurements with cases alone corresponded to each treatment of larvae and case together. In this way the oxygen consumption of the larvae was calculated by subtracting the oxygen uptake by cases alone from the corresponding oxygen uptake of cases with larvae inside. In the non-moving fluid treatment, five larvae in their cases were placed between two fine mesh (0.1 cm maximum pore size) double-layered screens positioned ~0.5 cm apart that spanned the inner diameter of the vial.

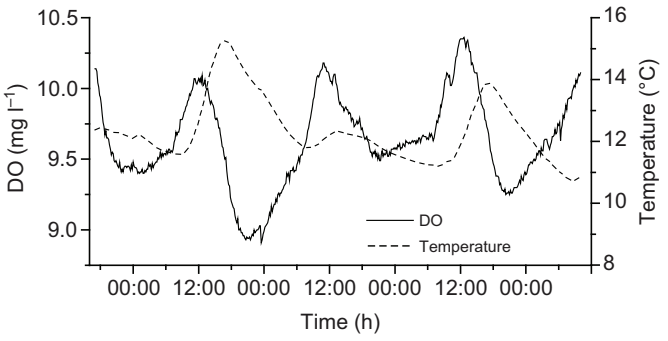

Fig. 2. Dissolved oxygen (DO) and temperature diel cycles in the upstream Valley Creek larval collection site from 17:00 h on 23 August to 10:00 h on 27 August 2012.

DO flux

DO flux, J ($mg m^{-2} s^{-1}$), across the larval case surface area, A (m^2), is defined as the rate of change (over time t) of the DO concentration, C ($mg l^{-1}$), within the sample volume, V (m^3):

$$\int_{A_t} -J \times \hat{n}\, dA = \int_{V_t} \frac{dC}{dt} dV , \quad (1)$$

where $\hat{n}$ is a vector of unit length normal to a plane tangent to the case surface and pointing away from the case, A_t is the cumulative case surface area, and V_t is the total water volume in the experimental set up. Integration leads to an expression for the total DO flux to the larvae:

$$J = \frac{V_t}{A_t} \frac{dC}{dt} . \quad (2)$$

For each experimental run, the rate of change of DO concentration (dC/dt) was estimated from the time series of measured DO concentrations, A_t was estimated by image processing analysis, and V_t was constant.

In our experimental set up, flux to a single larva and case can be considered a function of the following variables:

$$J = f_1(U, D, A_c, \rho) , \quad (3)$$

where f_1 is an unknown function, U is the discharge velocity ($m s^{-1}$), D is the molecular diffusion of oxygen ($m^2 s^{-1}$), A_c is the average larval case projected surface area (m^2) and ρ is the water density ($kg m^{-3}$). Using the Buckingham Π theorem for dimensional analysis (Buckingham, 1914) with five variables and three dimensions, when D, A_c and ρ are chosen as repeating variables, the following two dimensionless groups are formed:

$$\frac{J\sqrt{A_c}}{D\rho} = f_2\left(\frac{U\sqrt{A_c}}{D}\right), \quad (4)$$

where the denominator on the left side of equation, $D\rho/\sqrt{A_c}$, can be thought of as the transport of oxygen to the case surface area due to molecular diffusion. The Sherwood (Sh) number is the ratio of advective flux to molecular diffusive flux; therefore, $\sqrt{A_c}/D\rho$ can be interpreted as the Sh number. The bracketed term on the right of Eqn 4 can be interpreted as a Peclet number, which is a ratio between the diffusive (t_{diff}) and advective (t_{ad}) time scales:

$$Pe = \frac{t_{diff}}{t_{ad}} , \quad (5)$$

where $t_{diff}=A_c/D$ is the diffusion time (the time taken for DO to diffuse over an average larval case), and $t_{ad}=\sqrt{A_c}/U$ is the advective

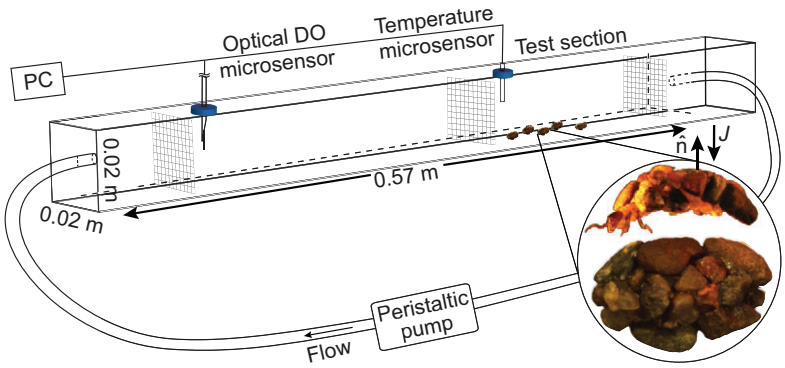

Fig. 3. Experimental set up with magnified side view of a *Glossossoma nigrior* larva extended from its case (above), and a case in plan view (below). *J*, DO flux; n̂, vector of unit length normal to a plane tangent to the case surface.

time (the time taken for DO to be advected by moving fluid over the length of a larval case of $\sqrt{A_c}$). Therefore, Eqn 5 becomes:

$$\mathrm{Pe} = \frac{t_{\mathrm{diff}}}{t_{\mathrm{ad}}} = \frac{U\sqrt{A_c}}{D}, \quad (6)$$

and Eqn 4 can be re-written as:

$$\mathrm{Sh} = f_2(\mathrm{Pe}). \quad (7)$$

Further explanation of these terms is included in the Discussion. The form of the unknown function f_2 is not known from dimensional analysis but is determined by the experimental data.

Larval oxygen consumption rates were converted from per area oxygen uptake across the case into units of DO consumption mg^{-1} larval tissue h^{-1} (Table 1). This conversion was carried out using the average plan view surface area of the cases of the Valley Creek larvae and the mean larval dry mass from 235 larvae from two northern California streams (0.404±0.93 mg) (C. McNeely, unpublished data). California larvae were collected from two streams in the Angelo Coast Range Reserve and were of the species *G. penitum* Banks (Fox Creek, *N*=193) and *G. califica* Denning (Elder Creek, *N*=42, where *N* represents the number of individuals of each species).

RESULTS

Respiration measurement

DO concentration time series normalized by the initial DO concentration for each experimental run with constant discharge and constant Pe are depicted in Fig. 4. Initial DO concentration, temperature and velocity were within the range of observed

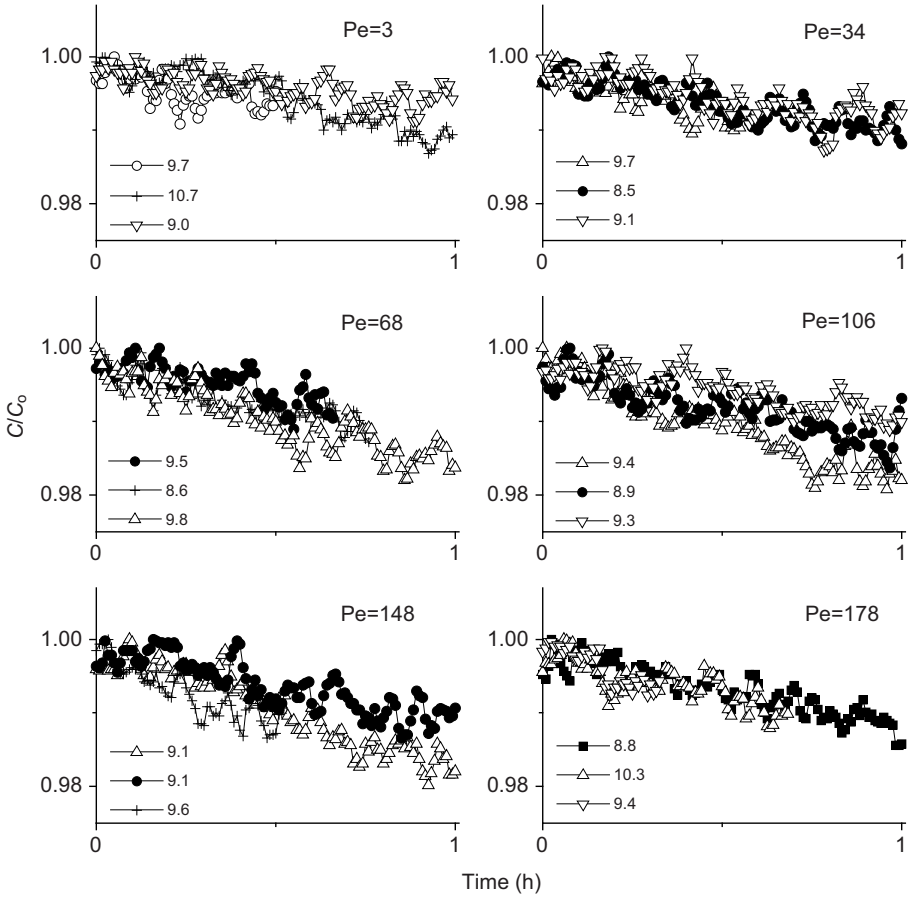

Fig. 4. Normalized DO concentration for larvae in their cases. C_o is the initial concentration of DO (mg l^{-1}). Data were sampled once every 30 s and averaged over a 2 min interval. Three example time series are presented from replicates of each treatment. Pe is the Peclet number (see Results). Numbers next to symbols represent C_o (mg l^{-1}).

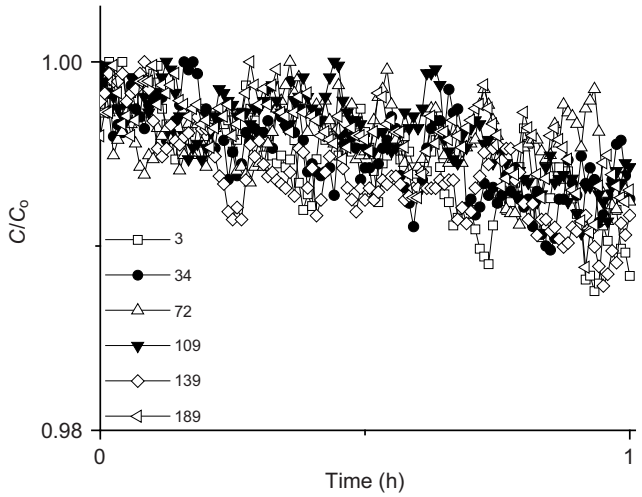

Fig. 5. Normalized DO concentration in the experimental chamber with empty *G. nigrior* cases. Numbers next to symbols represent Pe. For each Pe, one example time series is included.

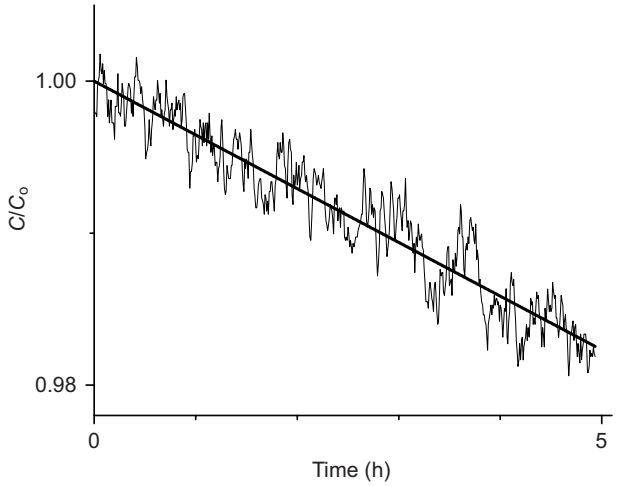

Fig. 6. Normalized DO concentration in a 120 ml vial with larvae in their cases in non-moving fluid; C_o=9.8 mg l^{-1} (y=1–0.004x).

corresponding variables in the field (Table 1). All DO concentrations decreased over time. The experimental set up was sealed, with constant temperature and therefore the decrease in DO concentration is attributed to larval respiration in the test section. The decrease of DO concentration was generally higher with increasing fluid flow velocities. For each specified discharge, each treatment was replicated at least three times and each time the set of larvae with their cases was replenished.

The normalized DO concentration time series for the cases alone is depicted in Fig. 5. At different fluid flow velocities and corresponding Pe number the decrease of DO concentration was similar. Therefore, all treatments were included on one plot, with one example curve for each treatment. Additionally, for Pe=34, only two cases-only DO time series were included in the larval flux calculations. Therefore, an average of these two case uptake rates corresponded with the third replicate of the larval uptake for this treatment. Because the quantity of interest is the oxygen drawdown slope rather than the absolute DO concentration, for comparison of the slopes among replicates within each Pe treatment, Figs 4 and 5 depict the oxygen concentrations normalized by the initial concentration (C_o). The comparison illustrates the variability of the drawdown slope for the treatments with larvae in their cases (Fig. 4) relative to the treatments without larvae, for which DO drawdown was nearly constant, independent of Pe (Fig. 5). Oxygen consumption for stagnant fluid in a 120 ml vial with larvae in their cases is shown in Fig. 6. The transport of DO to the larvae and cases was mostly, but not entirely, by molecular diffusion because there was still slight fluid motion resulting from larval movements. Normalized DO concentration shows a steady decrease at a much lower rate than in any other treatment in the presence of moving fluid.

DO flux

Mean (±s.d.) larval plan-view case area was 0.22±0.05 cm^2. The DO concentration time series (Figs 4–6) provided the basis for estimating an average rate of change of DO concentration (dC/dt) and corresponding flux of DO to larvae and their cases. Additionally, although the x-axis in Figs 4 and 5 stops at 1 h, to maximize statistical significance the longest available time period for each treatment was used for the calculation of the reported DO fluxes (Table 1). We included 49 individual treatments in our study. For nine of the 49 treatments, slopes from which dC/dt was calculated spanned multiple non-consecutive portions of individual Pe number treatments because of intervening temperature changes or other disturbances. In such treatments, the rate of change in DO concentration was an average of multiple slopes weighted by the duration of each contributing time series segment. The minimum time span for treatments using larvae in their cases was 0.3 h, the longest was 3.2 h, with an average of 1.0 h.

The flux of oxygen to the cases with larvae at different Pe numbers is depicted in Fig. 7 and Table 1. A prediction model similar to Michaelis–Menten kinetics fitted the data fairly well (r^2=0.76):

$$\mathrm{Sh} = 1 + \frac{\mathrm{Sh}_{\max}\,\mathrm{Pe}}{K_1 + \mathrm{Pe}} = 1 + \frac{6.8\,\mathrm{Pe}}{42 + \mathrm{Pe}}, \qquad (8)$$

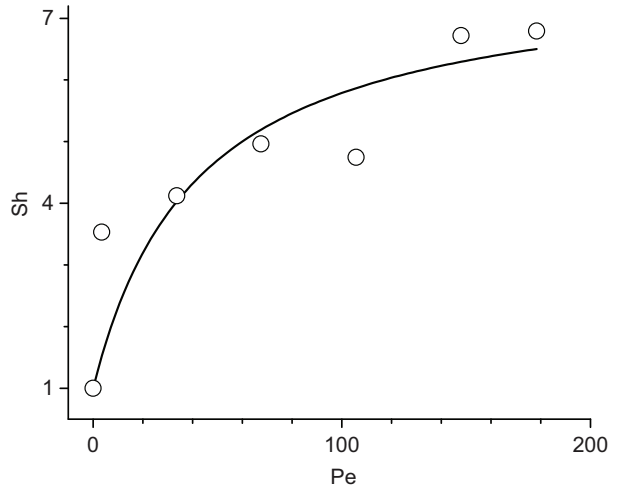

Fig. 7. The Sherwood number (Sh), which is the flux of DO in moving fluid (J_{LC}) normalized by DO flux in non-moving fluid (J_{LC_o}), *versus* Pe (Pe=$U\sqrt{A_c}/D$, where U is discharge velocity, A_c is larval case surface area and D is molecular diffusion of oxygen) for larvae in their cases for each experimental treatment. The form of the equation for the fitted line (Eqn 8; see Results) is similar to Michaelis–Menten kinetics, where Sh_{max}=6.8 is the maximum Sh value and K_1=42 is the Pe value corresponding to Sh=1+Sh_{max}/2.

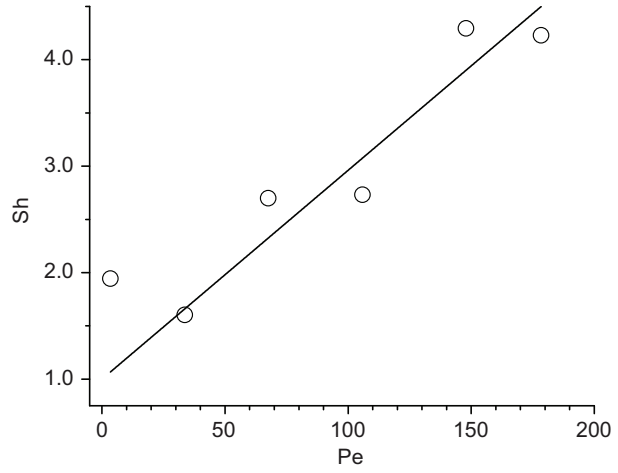

Fig. 8. DO flux to larvae (J_L) normalized by flux in a stagnant fluid (J_{LC_o}) *versus* Pe. The regression line is Sh=1+0.02Pe, r^2=0.91. J_L is the difference between DO flux to larvae with their cases and DO flux to the corresponding cases alone.

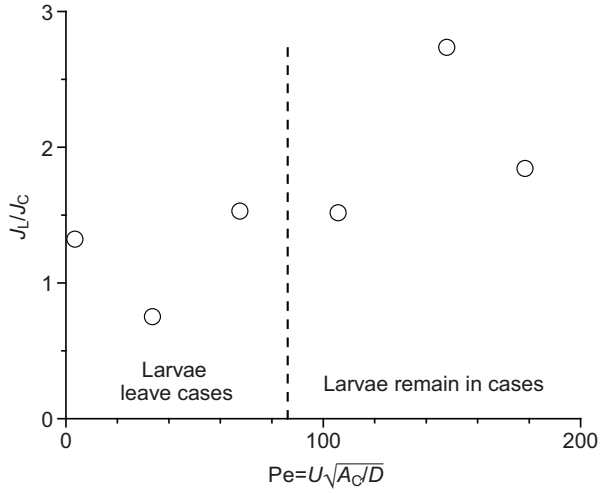

Fig. 9. The ratio of DO flux to *G. nigrior* larvae (J_L) divided by the corresponding flux of oxygen to the larval case (J_C).

where Sh_{max}=6.8 is the maximum Sh value and K_1=42 is the Pe value corresponding to Sh=1+Sh_{max}/2. Oxygen uptake by the larvae without cases is presented in Fig. 8. All fluxes were normalized by the oxygen flux to the larvae and cases in stagnant fluid (J_o). Figs 7 and 8 illustrate an increased larval DO consumption rate for increased discharge and corresponding velocities and Pe numbers. For DO flux to the larvae, a simple linear form of f_2 in Eqn 7 describes the trend fairly well, specifically:

$$Sh = 1 + 0.02\mathrm{Pe}, \quad (9)$$

with r^2=0.91.

The ratio of DO flux to the larvae alone over flux to the cases alone is presented in Fig. 9. When this ratio was unity, the case consumed the same amount of DO as the larva. Larval oxygen consumption rates were highest at the Pe of 178, which corresponded to a discharge velocity of 0.062 m s^{-1}. At Pe<87, larval consumption rates approached case consumption rates; larvae were occasionally observed abandoning their cases or extending from case openings. For Pe>87, larvae typically remained in their cases, with the exception of two out of 14 treatments for which Pe≥148.

DISCUSSION

Manipulation of fluid flow velocity while all other variables were held constant isolated the influence of fluid flow velocity on larval DO uptake and behavior. We expected to observe a higher respiration rate at higher water velocity, similar to the results of Feldmeth, who reported that oxygen consumption (mg g^{-1} dry mass h^{-1}) in the laboratory was greatest for caddisfly species (*Brachycentrus* spp.) at water velocities at which the species were found in the field (Feldmeth, 1970). Our data indicate a similar pattern (Table 1). Higher oxygen flux to larvae, which may be considered larval oxygen consumption, was associated with higher discharge velocities and higher Pe numbers as illustrated in Figs 7–9.

The positive relationship between flow rate and larval oxygen consumption is supported by the higher larval oxygen consumption in lotic compared with lentic flow conditions (Okano and Kikuchi, 2012). Oxygen consumption rate of *G. nigrior* measured in stirred vials from the Hirose River, Japan, was reported to be 11 mg O_2 mg^{-1} larval dry mass (Okano and Kikuchi, 2012). This is similar to the larval tissue consumption rate in our slower flow rate treatment (Table 1). To convert DO uptake per case area into consumption per mg larval tissue, we used larval dry mass available from California streams consisting of larvae from two different species but within the genus *Glossosoma*. Because the absolute quantity of oxygen consumed by larval tissue per time is not the focus of the study, but rather the relative oxygen consumption rate compared across multiple Pe treatments, the assumption was made that larval dry mass is of the same order of magnitude between the three species.

From studies of water-side mass transfer to macrophytes and to sediment, a general trend is apparent, specifically that increased velocity in the proximity of filaments increases the flux of a substance (Steinberger and Hondzo, 1999; Hansen et al., 2011). Our measurements support this pattern. In order to access oxygen-rich water, larvae must overcome the oxygen-depleted region surrounding them as well as that surrounding their cases. Under magnification of the cases in our study it was apparent that the stones that comprise *G. nigrior* cases as well as the silk filaments attaching the stones to one another were populated by micro-organisms, including diatoms that *G. nigrior* feed upon. Therefore, *G. nigrior* larval access to oxygen is limited not only by the physical boundary of the case stones but also by the respiration of the community of micro-organisms embedded in the case. Although food was not provided in the chambers, larvae were frequently observed clinging to other larval cases. Although this behavior was also observed in the field, albeit infrequently, access to the other larvae and their cases in each treatment introduced other variables into the system and weakened the conclusion about fluid flow effects on larval DO uptake and behavior.

Fluid flow velocity and water temperature mediate the water-side delivery of oxygen to aquatic organisms through turbulent mixing and diffusion, respectively. Regarding turbulent mixing, fluid motion imposes nearly constant time-averaged DO concentration in the proximity of an organism. Because of DO uptake by the organism, the constant concentration is reduced at the organism surface through a short distance with a steep DO gradient where the transport of DO is governed by molecular diffusion. More energetic turbulent mixing implies a steeper DO gradient in the proximity of the organism and therefore a large DO mass flux to the organism. A convenient quantification of mass flux to the

organism in a moving fluid could be expressed in terms of Sh and Pe. The Sherwood number has been used to relate fluid flow and mass transport to choral morphology (Helmuth et al., 1997) and epiphytic nickel uptake (Hansen et al., 2011). Dimensionless relationships that include Sh demonstrate the degree to which water motion and organism size affect mass transfer, and ultimately organism metabolic rate (Patterson, 1992). An example application of Pe is its use in describing lentic mass transport associated with lake metabolism (Antenucci et al., 2013).

With the objective of quantifying *G. nigrior* DO consumption, laboratory conditions were patterned after field conditions in Valley Creek. Rather than removing larvae from their cases and measuring respiration directly, larval oxygen consumption was calculated as the difference between consumption of larvae in their cases and consumption of cases alone. We endeavored to measure DO consumption of cased larvae because larvae were observed in their cases in the field.

Oxygen consumption slightly increased in nearly stagnant fluid at Pe=4 (Fig. 8). This can be explained by the possibility that larvae in the very slow fluid flow were actively seeking a more suitable hydraulic environment. *Glossossoma nigrior* larval behavior in the laboratory at the slower fluid flow velocities or in stagnant fluid may have been associated with drifting behavior in the field. Kohler and McPeek reported that drift increases at night because of case-building activity and associated vulnerability to erosion (Kohler and McPeek, 1989). However, under certain fluid flow conditions we observed that larvae arched their backs and extended their legs upward, behavior that would possibly increase the risk of larvae being swept up into the current. For comparison, mayfly nymphs with swimming ability actively enter the drift (Wiley and Kohler, 1980). No swimming ability was observed by the case-less, negatively buoyant *G. nigrior* larvae, but the arched and extended body posturing seems to indicate that under certain environmental conditions larval drift is not an entirely passive event. This possibility necessitates further research, but is not entirely unreasonable as body posture differences for active drift have been documented for stonefly larvae (Blum, 1989).

The benthic distribution of macroinvertebrates may be governed, in part, by the drifting activity as illustrated by the following examples. In marine environments, near-bed flow characteristics can strongly affect the settlement location of drifting invertebrates, especially for small organisms that are also weak swimmers (Stevenson, 1983; Butman, 1987; Mullineaux and Butman, 1991). This may be connected to chemical cues and the rate of turbulent mixing, which enable drifting organisms to detect waterborne chemical cues that provide information about bed suitability, such as benthic food resources or the presence of conspecifics (Patterson, 1992; Abelson, 1997).

Our study illustrates the influence of oxygen availability on *G. nigrior* behavior (Fig. 9). The implications of our results support the suggestion by Okano and Kikuchi that larval positioning on the stream bed is driven by oxygen requirements (Okano and Kikuchi, 2012). The results of this simplified laboratory study should be considered in light of the complex array of influencing factors and larval responses in the field. Nevertheless, this study contributes to understanding of the role of the larval *G. nigrior* case and under what conditions the case loses its functional benefit for the larva. The hydraulic environment in a natural or restored stream reach can be directly influenced by restoration practices or other anthropogenic influences. Understanding *G. nigrior* behavior at the lower extreme of fluid velocities in which larvae are observed in the field benefits river restoration and management decisions. Low DO availability to *G. nigrior* as a consequence of fluid flow conditions has a predictable effect on larval behavior.

LIST OF SYMBOLS AND ABBREVIATIONS

A	surface area
A_c	larval case surface area
A_t	cumulative surface area
C	dissolved oxygen concentration
C_0	initial dissolved oxygen concentration
DO	dissolved oyxgen
J_C	dissolved oxygen flux to cases alone
J_{LC}	dissolved oxygen flux to larvae with cases
l	length scale
n̂	vector of unit length normal to a plane tangent to the case surface
Pe	Peclet number
$\dot{Q}$	flow rate
Sh	Sherwood number
t	time
t_{ad}	advective time
t_{diff}	diffusion time
u	longitudinal velocity magnitude
u^*	shear velocity magnitude
U	discharge velocity
V	sample volume
V_t	total volume
z	distance above the stream bed
z_c	roughness crest elevation
ρ	water density

ACKNOWLEDGEMENTS

We thank the Belwin Conservancy for providing access to pristine *G. nigrior* habitat in Valley Creek, MN, USA.

AUTHOR CONTRIBUTIONS

Both M.W.L.M. and M.H. were involved in the conception of the study, the design of the experiments, interpretation of findings, and the writing of the manuscript. M.W.L.M. was responsible for the field and laboratory data collection.

COMPETING INTERESTS

No competing interests declared.

FUNDING

This work was supported by the National Science Foundation under grant IGERT: Nonequilibrium Dynamics Across Space and Time: A Common Approach for Engineers, Earth Scientists, and Ecologists [grant no. DGE-0504195]; the National Center for Earth-surface Dynamics (NCED), a Science and Technology Center funded by the office of Integrative Activities of the National Science Foundation [under agreement no. EAR-0120914]; as well as a 2012 summer fellowship from the University of Minnesota Civil Engineering Department.

REFERENCES

Abelson, A. (1997). Settlement in flow: upstream exploration of substrata by weakly swimming larvae. *Ecology* **78**, 160-166.

Antenucci, J. P., Tan, K. M., Eikaas, H. S. and Imberger, J. (2013). The importance of transport processes and spatial gradients on in situ estimates of lake metabolism. *Hydrobiologia* **700**, 9-21.

Blum, R. (1989). Drift postures of nemourid stonefly larvae (Insect, Plecoptera). *Aquat. Insects* **11**, 193-199.

Buckingham, E. (1914). On physically similar systems; illustrations of the use of dimensional equations. *Phys. Rev.* **4**, 345-376.

Butman, C. A. (1987). Larval settlement of soft-sediment invertebrates – the spatial scales of pattern explained by active habitat selection and the emerging role of hydrodynamical processes. *Oceanogr. Mar. Biol.* **25**, 113-165.

Eastham, L. (1939). Gill movements of nymphal *Ephemera* danica (Ephemeroptera) and the water currents caused by them. *J. Exp. Biol.* **16**, 18-33.

Feldmeth, C. R. (1970). The respiratory energetics of two species of stream caddis fly larvae in relation to water flow. *Comp. Biochem. Physiol.* **32**, 193-202.

Fenoglio, S., Bo, T., Czekaj, A. and Rościszewska, E. (2008). Feeding habits, fine structure and microhabitat preference of *Euthyplocia hecuba* (Hagen, 1861) (Ephemeroptera: Euthyplociidae) nymphs from Honduras. *Folia Biol. (Krakow)* **56**, 43-49.

Genkai-Kato, M., Mitsuhashi, I., Kohmatsu, Y., Miyasaka, H., Nozaki, K. and Nakanishi, M. (2005). A seasonal change in the distribution of a stream-dwelling stonefly nymph reflects oxygen supply and water flow. *Ecol. Res.* **20**, 223-226.

Hansen, A. T., Stark, R. A. and Hondzo, M. (2011). Uptake of dissolved nickel by *Elodea canadensis* and epiphytes influenced by fluid flow conditions. *Hydrobiologia* **658**, 127-138.
Helmuth, B., Sebens, K. and Daniel, T. (1997). Morphological variation in coral aggregations: branch spacing and mass flux to coral tissues. *J. Exp. Mar. Biol. Ecol.* **209**, 233-259.
Hynes, H. B. N. (1970). *Ecology of Running Waters*. Toronto: University of Toronto Press.
Kohler, S. L. and McPeek, M. A. (1989). Predation risk and the foraging behavior of competing stream insects. *Ecology* **70**, 1811-1825.
Kohler, S. L. and Wiley, M. J. (1997). Pathogen outbreaks reveal large-scale effects of competition in stream communities. *Ecology* **78**, 2164-2176.
Kovalak, W. P. (1976). Seasonal and diel changes in positioning of *Glossosoma nigrior* Banks (Trichoptera-Glossosomatidae) on artificial substrates. *Can. J. Zool.* **54**, 1585-1594.
Kwong, L., Mendez, P. K. and Resh, V. H. (2011). Case-repair in three genera of caddisflies (Trichoptera). *Zoosymposia* **5**, 269-278.
Lavandier, P. and Capblancq, J. (1975). Influence des variations d'oxygène dissous sur les invertébrés benthiques d'un ruisseau des Pyrénées Centrales. *Ann. Limnol.* **11**, 101-106.
Limm, M. P. and Power, M. E. (2011). The caddisfly *Dicosmoecus gilvipes*: making a case for a functional role. *J. North Am. Benthol. Soc.* **30**, 485-492.
McNeely, C., Finlay, J. C. and Power, M. E. (2007). Grazer traits, competition, and carbon sources to a headwater-stream food web. *Ecology* **88**, 391-401.
Mullineaux, L. S. and Butman, C. A. (1991). Initial contact, exploration and attachment of barnacle (*Balanus amphitrite*) cyprids settling in flow. *Mar. Biol.* **110**, 93-103.
Nikora, V., Goring, D., McEwan, I. and Griffiths, G. (2001). Spatially averaged open-channel flow over rough bed. *J. Hydraul. Eng.* **127**, 123-133.
Nikora, V., McEwan, I., McLean, S., Coleman, S., Pokrajac, D. and Walters, R. (2007). Double-averaging concept for rough-bed open-channel and overland flows: theoretical background. *J. Hydraul. Eng.* **133**, 873-883.
O'Donnell, B. C. (2009). Early nymphal development in ephoron leukon (Ephemeroptera: Polymitarcyidae) with particular emphasis on mouthparts and abdominal gills. *Ann. Entomol. Soc. Am.* **102**, 128-136.
Okano, J. and Kikuchi, E. (2012). Effect of current velocity and case adaptations on the distribution of caddisfly larvae (*Glossosoma*, Trichoptera). *Limnology* **13**, 37-43.
Okano, J., Kikuchi, E. and Sasaki, O. (2010). The role of particle surface texture on case material selection and silk lining in caddis flies. *Behav. Ecol.* **21**, 826-835.
Patterson, M. R. (1992). A mass transfer explanation of metabolic scaling relations in some aquatic invertebrates and algae. *Science* **255**, 1421-1423.
Raupach, M., Finnigan, J. and Brunet, Y. (1996). Coherent eddies and turbulence in vegetation canopies: the mixing-layer analogy. *Boundary-Layer Meteorol.* **78**, 351-382.
Scott, D. (1958). Ecological studies on the Trichoptera of the River Dean, Cheshire. *Arch. Hydrobiol.* **54**, 340-392.
Statzner, B. and Doledec, S. (2011). Mineral grain availability and pupal-case building by lotic caddisflies: effects on case architecture, stability and building expenses. *Limnologica* **41**, 266-280.
Steinberger, N. and Hondzo, M. (1999). Diffusional mass transfer at sediment-water interface. *J. Environ. Eng.* **125**, 192-200.
Stevenson, R. (1983). Effects of current and conditions simulating autogenically changing microhabitats on benthic diatom immigration. *Ecology* **64**, 1514-1524.
Tindall, M. and Kovalak, W. (1979). Food particle size consumed by larval *Glossosoma nigrior* (Trichoptera: Glossosomatidae). *Great Lakes Entomol.* **12**, 105-108.
Wiggins, G. B. (2004). *Caddisflies: the Underwater Architects*. Toronto: University of Toronto Press.
Wiggins, G. B. and Wichard, W. (1989). Phylogeny of pupation in Trichoptera, with proposals on the origin and higher classification of the order. *J. North Am. Benthol. Soc.* **8**, 260-276.
Wiley, M. J. and Kohler, S. L. (1980). Positioning changes of mayfly nymphs due to behavioral regulation of oxygen consumption. *Can. J. Zool.* **58**, 618-622.
Zimmerman, J. K. H. and Vondracek, B. (2007). Brown trout and food web interactions in a Minnesota stream. *Freshw. Biol.* **52**, 123-136.